

# Advanced Materials Interfaces

## Bio-mimetic locomotion on water of a porous natural polymeric composite

--Manuscript Draft--

<b>Manuscript Number:</b>	admi.201500373
<b>Full Title:</b>	Bio-mimetic locomotion on water of a porous natural polymeric composite
<b>Article Type:</b>	Full Paper
<b>Keywords:</b>	Self-Motors, Bio-locomotion, Bio-mimetics, Marangoni effect, Surface tension gradient.
<b>Corresponding Author:</b>	Ioannis Liakos Istituto Italiano di Tecnologia Genova, ITALY
<b>Additional Information:</b>	
<b>Question</b>	<b>Response</b>
<b>Corresponding Author Secondary Information:</b>	
<b>Corresponding Author's Institution:</b>	Istituto Italiano di Tecnologia
<b>Corresponding Author's Secondary Institution:</b>	
<b>First Author:</b>	Ioannis Liakos
<b>First Author Secondary Information:</b>	
<b>Order of Authors:</b>	Ioannis Liakos Pietro Salvagnini Elisa Mele Riccardo Carzino Alice Scarpellini Athanasia Athanassiou
<b>Order of Authors Secondary Information:</b>	
<b>Abstract:</b>	<p>Observation of the natural world can provide invaluable information on the mechanisms that semi-aquatic living organisms or bacteria use for their self-propulsion. Microvelia, for example, uses wax excreted from its legs to move on water in order to escape from predators or reach the bank of the river. Mimicking such mechanism, few self-propelled materials on water, as camphor, have been previously developed, but weak points like slow locomotion, short movement duration or shape-restrictions still need to be improved. Herein we present a totally green self-assembled porous system, formed by the combination of a natural polymer with an essential oil, that spontaneously moves on water for hours upon expulsion of the oil, with high velocities reaching 15 cm/s. The structural characteristics of the natural polymeric composite are carefully analyzed and associated to its spontaneous movement. Surface tension change experiments are also presented that connect the essential oil release with the locomotion of the porous composite films. This research work opens novel routes towards bio-inspired natural materials that can be used for mimicking and studying the motion of bio-organisms and microorganisms, and for applications such as energy harvesting, aquatic pollution monitoring, drug delivery, to name few.</p>

1  
2  
3  
4  
5 DOI: 10.1002/  
6

7 **Article type:** Full paper  
8

9 **Bio-mimetic locomotion on water of a porous natural polymeric composite**  
10  
11

12  
13 *Ioannis Liakos\**, *Pietro Salvagnini*, *Elisa Mele*, *Riccardo Carzino*, *Alice Scarpellini*, *Athanassia*  
14 *Athanassiou\**  
15

16  
17  
18 Dr. I. Liakos, Dr. E. Mele, Dr. R. Carzino, Dr. A. Athanassiou  
19

20  
21 Smart Materials, Istituto Italiano di Tecnologia (IIT), via Morego 30, 16163 Genova, Italy.  
22

23 Emails: [ioannis.liakos@iit.it](mailto:ioannis.liakos@iit.it), [athanassia.athanassiou@iit.it](mailto:athanassia.athanassiou@iit.it)  
24

25 Dr. Pietro Salvagnini  
26

27  
28 Pattern Analysis and Computer Vision, Istituto Italiano di Tecnologia (IIT), via Morego 30, 16163  
29 Genova, Italy.  
30

31 Dr. A. Scarpellini  
32

33  
34 Nanochemistry, Istituto Italiano di Tecnologia (IIT), via Morego 30, 16163 Genova, Italy.  
35  
36  
37

38  
39 **Keywords:** Self-Motors, Bio-locomotion, Bio-mimetics, Marangoni effect, Surface tension gradient.  
40  
41

42  
43  
44 Observation of the natural world can provide invaluable information on the mechanisms that semi-  
45 aquatic living organisms or bacteria use for their self-propulsion. *Microvelia*, for example, uses wax  
46 excreted from its legs to move on water in order to escape from predators or reach the bank of the river.  
47  
48 Mimicking such mechanism, few self-propelled materials on water, as camphor, have been previously  
49 developed, but weak points like slow locomotion, short movement duration or shape-restrictions still  
50 need to be improved. Herein we present a totally green self-assembled porous system, formed by the  
51 combination of a natural polymer with an essential oil, that spontaneously moves on water for hours  
52 upon expulsion of the oil, with high velocities reaching 15 cm/s. The structural characteristics of the  
53  
54  
55  
56  
57  
58  
59  
60  
61  
62  
63  
64  
65

1  
2  
3  
4  
5 natural polymeric composite are carefully analyzed and associated to its spontaneous movement.  
6  
7 Surface tension change experiments are also presented that connect the essential oil release with the  
8  
9 locomotion of the porous composite films. This research work opens novel routes towards bio-inspired  
10  
11 natural materials that can be used for mimicking and studying the motion of bio-organisms and  
12  
13 microorganisms, and for applications such as energy harvesting, aquatic pollution monitoring, drug  
14  
15 delivery, to name few.  
16  
17  
18  
19  
20  
21

## 22 **1. Introduction**

23  
24 Motion of biological systems can be induced from non-equilibrium conditions, related to physical or  
25  
26 chemical instabilities.<sup>[1, 2]</sup> When the driving force is the surface tension gradient created at the edges of  
27  
28 floating systems in contact with water, then the movement is explained by the so-called “Marangoni  
29  
30 effect”.<sup>[3-6]</sup> Non-biological self-propelled systems based on this effect have also been developed, with  
31  
32 the most studied one being the camphor that shows spontaneous movement on the air/water interface.<sup>[1,</sup>  
33  
34 <sup>7-25]</sup> Other self-motors with propelling function based on the same principle have been reported and can  
35  
36 be used for environmental,<sup>[11, 26]</sup> drug delivery,<sup>[25]</sup> lab-on-a-chip or energy harvest applications.<sup>[13, 21, 23,</sup>  
37  
38 <sup>24]</sup> The maximum recorded velocity of a camphor disk on the air/water interface has been  
39  
40 approximately 6 cm/s<sup>[10]</sup> with the duration of the motion lasting few seconds. Disk-shaped gel particles  
41  
42 formed from camphor, agarose and PDMS were also developed for spontaneous locomotion at the  
43  
44 air/water interface<sup>[22]</sup> with maximum velocity 2 cm/s. A different than camphor system that has been  
45  
46 reported was based on a 1,10-phenanthroline disk moving on divalent metal ion aqueous solutions,  
47  
48 where the velocity of the disk ranged from 10 to less than 3 cm/s depending on the metal ions.<sup>[15]</sup>  
49  
50 Another reported system was made of self-assembled peptides incorporated into a metal-organic  
51  
52 framework and released upon contact with water, causing a propulsion with velocity between 4.5 and  
53  
54 8.5 cm/s for few minutes.<sup>[27]</sup> In an alternative approach the supply of ethanol to a tank reservoir on the  
55  
56  
57  
58  
59  
60  
61  
62  
63  
64  
65

1  
2  
3  
4  
5 top of a nanocellulose film provided surface tension gradient on the water surface, responsible for the  
6  
7 movement of the film for 74 m at a velocity of nearly 2 cm/s (~ 1 hour movement).<sup>[9]</sup> Additionally,  
8  
9 lithographically structured poly-N-isopropylacrylamide (PNIPAm) gels soaked in ethanol and then  
10  
11 placed on water have shown velocities of 17-39 cm/s depending on the shape and size of the gel.<sup>[7]</sup>  
12  
13  
14 Similar velocities (30 cm/s) have been also reached with microflotillas consisting of various SU-8  
15  
16 microboats filled with isopropyl alcohol and linked with a Nylon rope.<sup>[12]</sup> An overall review of the  
17  
18 various self-propelled systems (either those where the propellant container was at the same time the  
19  
20 propelled object or the ones where the propellant was placed in a reservoir) and their velocities is well  
21  
22 described in the work of Pimienta and Antoine.<sup>[28]</sup>  
23  
24  
25  
26

27 Here, we present the realization of a new self-propelled system consisting of cellulose acetate  
28  
29 (CA) and peppermint (PM) essential oil. Disc-shaped objects of few millimeters diameters made of this  
30  
31 natural composite are capable of producing significant mechanical work on the air/water interface for  
32  
33 few hours. In particular, upon contact with water the presented natural composites start expelling the  
34  
35 contained essential oil changing their composition in a dynamic way. The movement of the system is  
36  
37 due to imbalance of forces parallel to the water surface, because of differences of surface tension  
38  
39 created at the margins of the samples due to the essential oil expel. Apart from the PM essential oil  
40  
41 release in water, also its simultaneous partial evaporation in air is responsible for the surface tension  
42  
43 gradients created at the edges of the floating object at the air/water interface. The Marangoni flow that  
44  
45 pulls the composites from their position occurs from the lower (expelled essential oil) to the higher  
46  
47 (water) surface tension areas.<sup>[29]</sup> The composite developed in this work has many advantages compared  
48  
49 to other systems since it is totally natural and inexpensive, self-assembles into a porous structure, can  
50  
51 be used as self-standing material or as coating on devices, its direction of motion can be selected by  
52  
53 modifying its shape, its propulsion can have very long duration and reaches velocities higher than 10  
54  
55 cm/s.  
56  
57  
58  
59  
60  
61  
62  
63  
64  
65

## 2. Methods and Results

### 2.1 Composite Material Development

Free-standing composite films of CA and PM essential oil were developed as described in the experimental part and subsequently were accurately cut in disc shapes of 14 mm diameter, 55  $\mu\text{m}$  thickness and 10 mg weight. The calculated amount of PM oil inside the Motor was 6.7  $\mu\text{g}$ . The CA-PM essential oil disc Motors attain a whitish color, different than the transparent bare CA film (**Figure 1a**), due to light scattering effects caused by their structure, that will be analyzed further down. The Motors are flexible (Figure 1b) and are floating on water (Figure 1c). Investigations by atomic force microscope (AFM) revealed the presence of distinct spherical domains of approximately 10  $\mu\text{m}$  in diameter exposed on the surface of the polymer matrix (Figure 1d,e). This is also confirmed by scanning electron spectroscopy (SEM) images, where the porosity of the samples is clearly visible not only on the surface (Figure 1f) of the films, but also throughout their volume (Figure 1g). This porosity is responsible for the whitish color of the composite samples due to light scattering. The reason of the formation of this porous structure is the spontaneous phase separation between the PM essential oil and the CA polymer, causing the creation of PM microspheres throughout the polymer volume. During the drying of the films, acetone, the volatile co-solvent of the two components of the samples evaporates, and the oil micro-droplets remain as filled pores in the matrix. Therefore, all the pores revealed during the AFM and SEM investigation are filled with the PM essential oil.

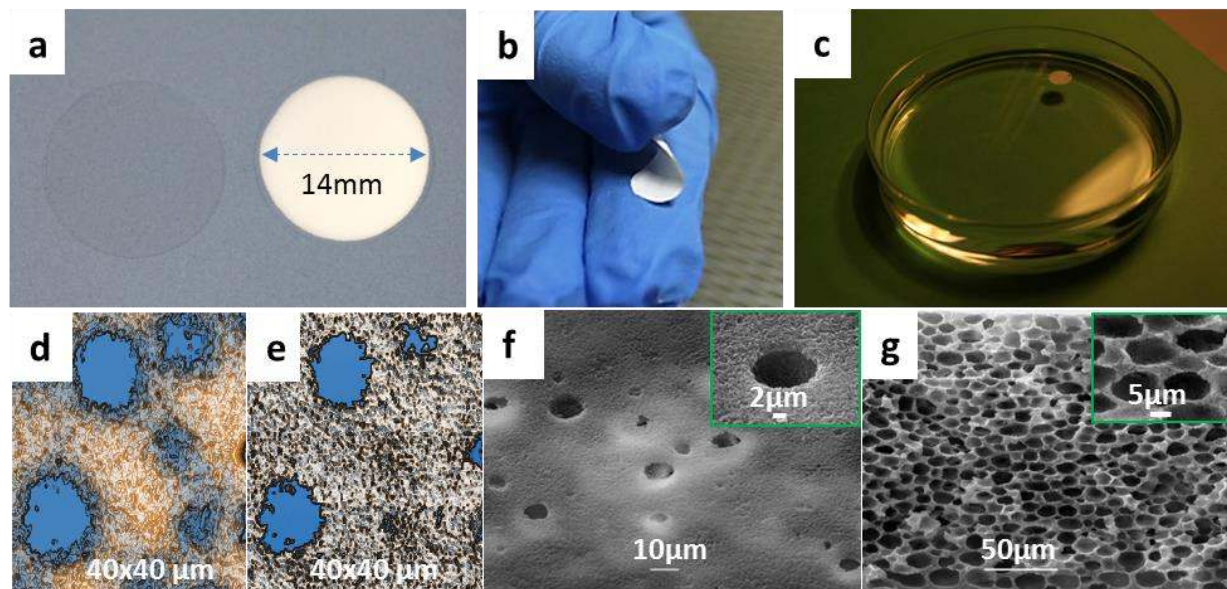


**Figure 1** Demonstration of the Motors and their topography. **a**, Comparison between bare CA (left) and CA-PM Motor (right) film. **b**, Demonstration of the flexibility of the disc Motor. **c**, Photograph showing the Motor floating on water. **d**, Topography AFM image of the surface of a Motor. **e**, Phase AFM image of the surface of a Motor. **f**, Surface SEM image of a Motor and a zoom in a pore for better visualisation (inset). **g**, Cross-section SEM image of a Motor and a higher magnification zoom (inset).

## 2.2 Self-propulsion on Water

Upon placement of the microporous disc-shaped Motors on the water surface, they exhibit intense and variable propulsion. The locomotion of the disc Motors, has been recorded using a video camera and analyzed using recognition and edge detector techniques.<sup>[30-33]</sup> The analyzed motion of one Motor shown in **Figure 2**, demonstrates different motion patterns on the water, varying between asymmetric (both axes of motion were irregular) (Figs 2a, 2c and 2d) and symmetric (one of the two axes was constant) (Figure 2b) and between continuous (Figure 2a) and intermittent (Figure 2d). In general, arbitrary motion of the Motors can be attributed to increased excretion of the essential oil from

1  
2  
3  
4  
5 selected sites of the Motor with respect to others that changes dynamically, due to structural variations  
6  
7 in the films, creating varying surface tension barriers at the Motors' edges that need to be overcome  
8  
9 from the Motors in order to move, all phenomena that will be further analyzed next. The position of the  
10  
11 Motor versus time is plotted in Figure 2e for the whole motion duration, where it can be seen that for  
12  
13 most of the time the motion was quite regular and was happening on average around all the area of the  
14  
15 14 cm-diameter Petri dish. Only in the beginning (0-320 s) and towards the end, after approximately  
16  
17 8200 s, the motion appeared more random and localized at one side of the Petri dish. In the latter case  
18  
19 the motion becomes localized due to reduced mobility of the Motor, whereas in the former case the  
20  
21 reason can be connected to the highly irregular essential oil release at early times. In Figure 2f is shown  
22  
23 the position versus time of the Motor with respect to the center of the Petri dish for these early  
24  
25 locomotion times (first 320 s), where are highlighted with yellow the time intervals illustrated in Figure  
26  
27 2a, 2b and 2c. The relative graphs of position versus time for all Figures 2a-2d are shown in the  
28  
29 supporting information (**Figure S1**).

30  
31  
32  
33  
34  
35  
36  
37 The velocity of the Motor in both x and y directions reaches its maximum values, close to 15  
38  
39 cm/s, in the time period between about 700 s (12.5 min) and 1500 s (25.0 min) of the propulsion  
40  
41 (Figure 2g). This velocity is higher than those of other reported Motors where, as in our case, the  
42  
43 material is the propelled object itself. For example, the velocity of a representative camphor on water  
44  
45 was about 4 cm/s<sup>[28, 34]</sup> and of a metal organic framework that was releasing peptides onto the water-air  
46  
47 interface from 2 to 8 cm/s for few minutes<sup>[27]</sup>. Interestingly, the disc was rotating both clockwise and  
48  
49 anticlockwise (supporting information **Figure S2**), another indication of uneven distribution of the  
50  
51 expelled essential oil along the disc periphery, with the average module of rotation velocity oscillating  
52  
53 between 10 – 20 rpm approximately (supporting information **Figure S3**). From the translational  
54  
55 velocity (Figure 2g), the angular velocity (Figure S3) and knowing the mass (0.01 g) and the inertia of  
56  
57 the disc Motor it was possible to estimate its kinetic energy, that is plotted in Figure 2h. It can be  
58  
59  
60  
61  
62  
63  
64  
65

1  
2  
3  
4  
5 noticed that the maximum kinetic energy was not obtained at the very beginning but after almost 13  
6  
7 minutes (778 s) from the initiation of the motion. This time is most likely related to the maximization  
8  
9 of the essential oil release rate from the CA matrix. Indeed after about 13 min of locomotion the  
10  
11 number of discrete movements of the Motor is maximum, and subsequently it decreases with time  
12  
13 gradually, as shown in Figure 2i. The cumulated overall distance travelled by the Motor was calculated  
14  
15 integrating the velocity of the Motor (Figure 2g) and is shown in Figure 2j. After 3 h the disc, that  
16  
17 contained 6.7 mg of PM, had travelled more than 77 m, a much higher distance than the one travelled  
18  
19 by camphor boats (millimetres or centimetres),<sup>[1, 28, 34]</sup> by polymeric capsules with organic solvents (25  
20  
21 m)<sup>[35]</sup> and by flotilla boats with isopropyl alcohol reservoir (1 m)<sup>[12]</sup>. In the work of metal organic  
22  
23 framework the amount of peptides used as a fuel was varying between 234 and 702 mg and the  
24  
25 framework was propelled with velocities ranging from 2 to 8 cm/s for 5-15 min depending on the  
26  
27 amount of peptides<sup>[27]</sup>. In another work, 5  $\mu$ l of a polysulfone in N,N-dimethylformamide (DMF)  
28  
29 solution was placed on a water surface and solidified creating porous polymer capsules. The DMF was  
30  
31 slowly released ranging the velocity between 11.4 – 15.7 cm/s and for a distance of 24.52 m.  
32  
33  
34  
35  
36  
37  
38  
39  
40  
41  
42  
43  
44  
45  
46  
47  
48  
49  
50  
51  
52  
53  
54  
55  
56  
57  
58  
59  
60  
61  
62  
63  
64  
65



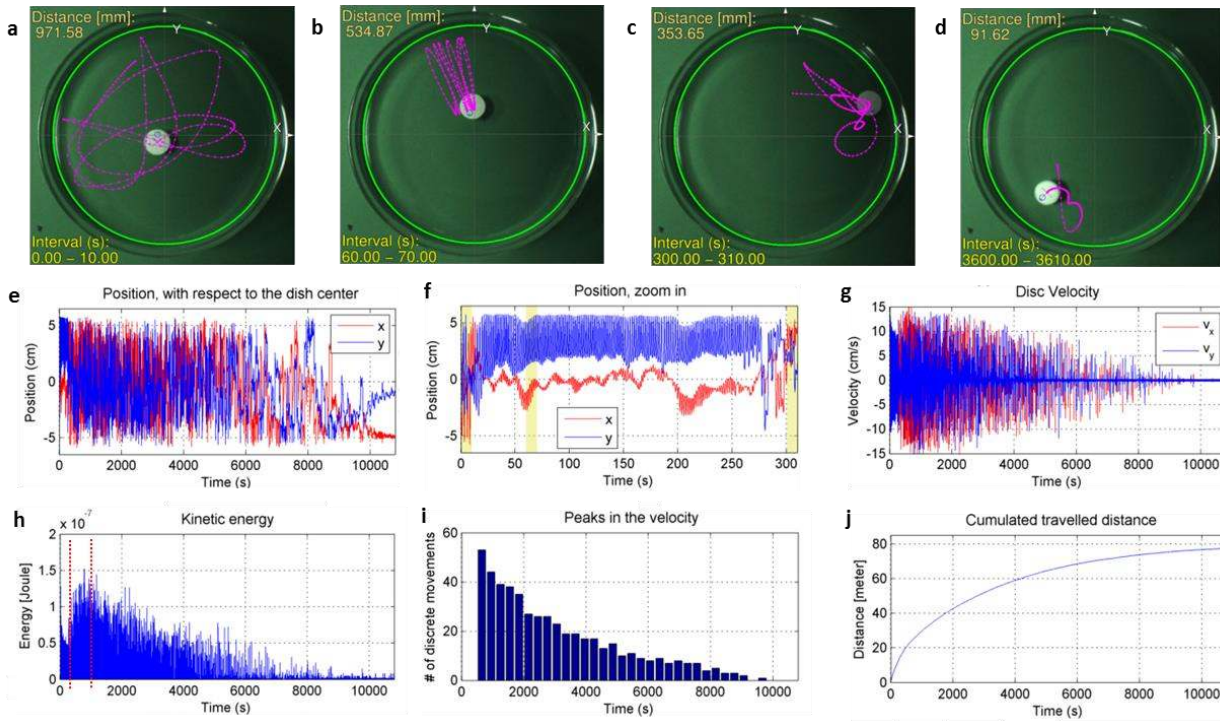


**Figure 2** Motion analysis of disc Motor. **a-d**, Locomotion of Motor and trajectory of its motion (pink line) at different time intervals of 10 s from the beginning of the experiment until 1 h and 10 s. **e**, Position versus time of the Motor with respect to the centre of the Petri dish and along the x and y directions. **f**, Zoom of the position of the Motor versus time for the first 320 s, where the highlighted yellow zones correspond to the trajectory motions shown in a, b and c. **g**, Instantaneous (computed between 3 consecutive frames) velocity of the disc motor from the centre of the Petri dish and along the two axes during time. **h**, Kinetic energy of the Motor, both from disc translation and disc self-rotation. **i**, Number of distinct motions of 5 min intervals. **j**, Cumulated distance travelled by the Motor versus time.

The motion termination of the CA-PM Motor can be related to both the total expulsion of the essential oil from the porous composite and the saturation of the surface tension. The second hypothesis

1  
2  
3  
4  
5 was verified in this work since for all the experiments performed onto the confined water surface, after  
6  
7 the end of the propulsion effect, the samples were able to continue the movement when they were put  
8  
9 onto fresh water. This demonstrates that even if a part of the released essential oils evaporates, the  
10  
11 substances remaining onto but also dissolved into the water would eventually minimize the surface  
12  
13 tension differences between the expelled oil and the liquid on which the Motor floats, preventing the  
14  
15 locomotion of the latter. Two videos (see supporting materials Video S1) show the aged disc-shaped  
16  
17 Motor after 2 h and after 1 day locomotion on water, respectively, dried and placed onto fresh water  
18  
19 (note that disc Motors might need to be flatten on the water prior to their movement, since they were  
20  
21 slightly bended when dried). The videos of selected intervals of the Motor are presented in the  
22  
23 supporting information (Videos S2-S8). During the first phase of the experiment (before removal from  
24  
25 the water and drying) the motion of the Motor after 2 hours was very slow with velocity from 0 – 60  
26  
27 mm/s and just 3 intermittent movements within 2 min (Video S8), whereas after one day the sample  
28  
29 appeared immobile. Inversely, the Motor previously left for 2 h on water, after being dried and  
30  
31 repositioned on fresh water, was able to move again in a continuous way (Video S1 – left part of the  
32  
33 video) for the first minutes and intermittently afterwards, completing its motion after 1600 s (27 min)  
34  
35 approximately. Noticeably the motion was always regular following the path of boundaries of the Petri  
36  
37 dish, most probably due to the low amount of remaining PM in the CA matrix that was continuously  
38  
39 released towards one side indicated by the motion direction. The aged Motor previously left for 1 day  
40  
41 on water was able to perform just few small movements on the fresh water (Video S1 – right part of the  
42  
43 video) since most of its pores, previously containing the essential oil, were already open, as is  
44  
45 described below in the SEM analysis section.  
46  
47  
48  
49  
50  
51  
52  
53  
54  
55  
56  
57  
58

### 59 **2.3 Mechanism of Locomotion**

60  
61  
62  
63  
64  
65

1  
2  
3  
4  
5 In **Figure 3** the SEM topography of the Motors before and after the propulsion are illustrated. The  
6  
7 number of open surface pores considerably increased after 1 day of Motor floating on the water (Figure  
8  
9 3a and 3b). Figure 3c shows a slightly-open pore of an as-prepared Motor, whereas Figure 3d shows an  
10  
11 open pore after 1 day of the Motor on water, indicating how a closed pore can become open after the  
12  
13 excretion of the essential oil onto the water. It was noted that some of the pores were already open  
14  
15 before deposition of the Motor on the water surface (Figure 3a and 3e). The release of the oil after the  
16  
17 contact of the composite films with the water can be attributed to the slightly hygroscopic character and  
18  
19 therefore swelling of the matrix of the Motor that might cause the opening of the pores releasing the  
20  
21 entrapped essential oil (schematically illustrated in Figure 3f, showing also the expected volatility of  
22  
23 PM oil). As shown before, both the velocity and the kinetic energy of the Motors need few minutes to  
24  
25 arrive to their maximum, and during these initial minutes the motion of the Motors is more confined  
26  
27 with respect to consequent times (Figure 2e). These minutes most likely coincide with the time needed  
28  
29 for the optimization of the swelling of the matrix, and thus the maximization of the release rate of  
30  
31 essential oil out of it. Water contact angle measurements (WCA) on the Motors' surface before and  
32  
33 after the end of their locomotion revealed that they have a very hydrophilic character in the first case  
34  
35 while they become quite hydrophobic in the second (supporting information **Figure S4**). This increase  
36  
37 in hydrophobicity is most likely due to opening of the pores of the film during the locomotion releasing  
38  
39 the essential oil. At the end of the locomotion and after drying of the Motors at ambient atmosphere the  
40  
41 air trapped inside the open pores can increase dramatically their surface hydrophobicity.<sup>[36]</sup>  
42  
43  
44  
45  
46  
47  
48  
49  
50  
51  
52  
53  
54  
55  
56  
57  
58  
59  
60  
61  
62  
63  
64  
65

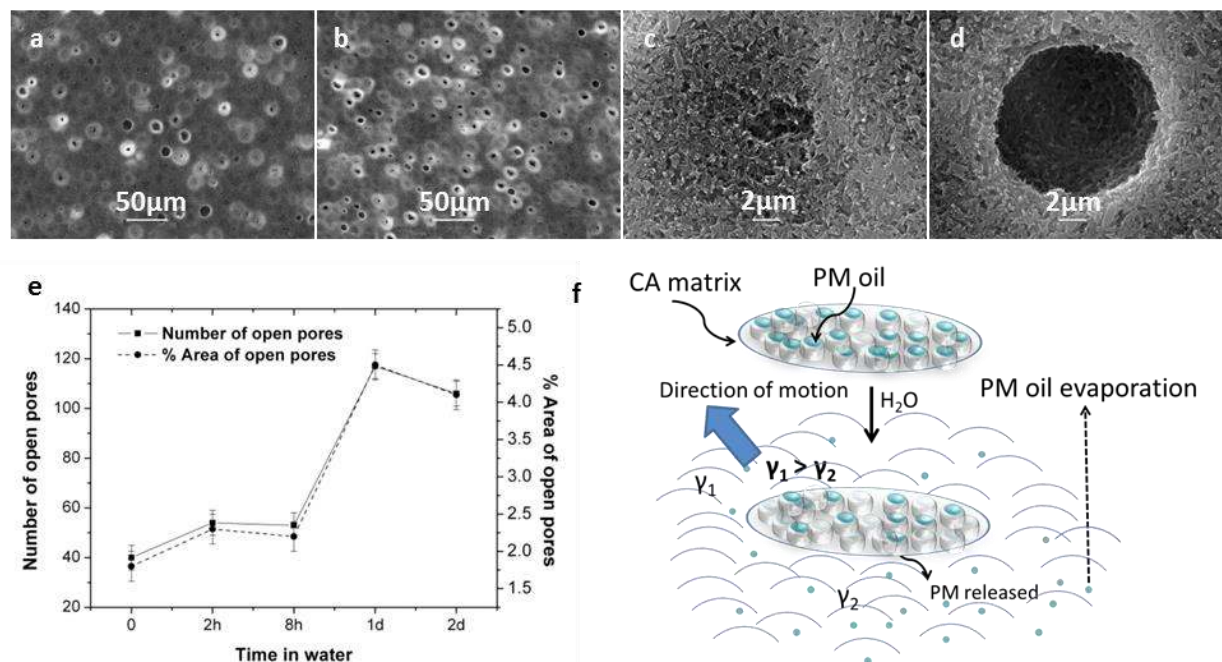


**Figure 3** Release of PM oil from the Motor on water and mechanism of locomotion. **a**, SEM of the surface of an as-prepared Motor. **b**, SEM of the surface of the same Motor after 1 day on water. **c**, SEM of a slightly open pore at the surface of an as-prepared Motor. **d**, SEM of an open pore at the surface of the Motor after 1 day on water. **e**, Number of pores and their % area with respect to the area of the matrix calculated using ImageJ analysis from SEM images taken at different times of the Motor on the air/water interface. **f**, Schematic illustration of PM oil release/evaporation and surface tension gradient mechanism ( $\gamma_1 > \gamma_2$ ) that describes the phenomenon of the Motor motion.

To explain in detail the locomotion mechanism, changes in the water surface tension were measured using a Langmuir-Blodgett (LB) tensiometer after placing the Motor on the surface of 200 ml of water in a Petri dish of 14 cm diameter. It is expected that as soon as the Motor comes in contact with the water the PM essential oil starts being released decreasing the surface tension of water, since PM has much lower surface tension (approximately 27 mN/m) than water (72mN/m).<sup>[37]</sup> The changes in the surface tension do not depend only on the essential oil release but on a combination of subsequent

phenomena, like PM evaporation and dilution, since it is well known that EOs consist of many volatile, and few water soluble chemical compounds.<sup>[38]</sup>

The change in the surface tension ( $\pi(t)$ ) that in the bibliography is often found as surface pressure<sup>[39, 40]</sup> is given by the Equation 1:

$$\pi(t) = |\gamma_0 - \gamma(t)| \quad (1)$$

where  $\gamma_0$  is the surface tension of pure water and  $\gamma(t)$  is the surface tension related to the essential oil's release, evaporation and dissolution. After the placement of the Motor on the water surface, the change of surface tension increased rapidly reaching about 2mN/m in 700 s (**Figure 4a** and **Figure S5** in supporting information). After the first 700 s, the variation in the surface tension with respect to the initial water surface tension started decreasing slowly showing sharp peaks with decreasing frequency in time (Figure 4c) until approximately 8000 s. After that, the peaks' occurrence stopped almost completely, and the change in surface tension reached eventually the value 1.25 mN/m approximately after 3 h. The monitored peaks are most likely related to water-induced disturbances to the probe of the tensiometer due to the discrete movements of the Motor, indicating change in the direction of the motion, triggered by essential oil accumulation at a specific sample side. Indeed, in Figure 2i presented above it is clearly demonstrated that the number of discrete motions of the Motor is minimized after 8000 s. Moreover, comparing the behavior of the surface tension change vs. time (Figure 4a) with that of the Motor's kinetic energy vs time presented above (Figure 2h) it can be seen that the maximum values in both cases are reached approximately 700 s after the initiation of the Motor's motion, verifying that the motion of the Motor depends on the changes of the surface tension at its borders induced by essential oil release. As expected, the control experiment with the CA disc without the PM essential oil placed on water, showed that the variation of surface tension remained zero with just a small peak due to the disturbance of the water surface upon placement (Figure 4a blue line).

1  
2  
3  
4  
5 The combinatory effect of the sequential or parallel events of the essential oil-release from the  
6  
7 CA matrix, its partial evaporation, and dissolution, is responsible for the dynamic change of the surface  
8  
9 tension of the liquid on which the Motor is moving. Even after 3 h of motion (Figure 4a) the surface  
10  
11 tension has not reached a stable value. This dynamic change is responsible for the prolonged movement  
12  
13 of the CA-PM Motors, since as long as the surface pressure is not stabilized the propulsion continues.  
14  
15 Indeed, in the case of camphor boats<sup>[41, 42]</sup> or soaps<sup>[43]</sup> the surface pressure reaches rapidly a plateau  
16  
17 resulting in their short motion duration (seconds or minutes). Comparing the camphor and the soap  
18  
19 systems, the use of the first saturates faster the surface with surfactants than the more volatile camphor,  
20  
21 making the motion of the second to last longer<sup>[44]</sup>.  
22  
23  
24  
25  
26

27 Figure 4b, that shows in detail the changes in surface tension for the first 300 s of motion of the  
28  
29 composite Motor, reveals that during this time this change increases in a continuous, undisturbed way.  
30  
31 Figs. 4c, d instead show in detail the changes in surface tension for later times of the motion and  
32  
33 demonstrate that the surface tension variation shows repeated “spikes” with decreasing frequency as  
34  
35 the time passes. As mentioned above, the “spikes”, that start to occur after 300 s of motion, represent  
36  
37 discrete movements of the natural composite, since they result from the perturbation on the water  
38  
39 surface every time the Motor changes direction. The “spikes” reveal a motion of the Motor with  
40  
41 increased intensity after 300 s, exactly as described above in the Figure 2. This most likely occurs  
42  
43 because the CA matrix needs this initial time to swell by water, releasing after the swelling in a more  
44  
45 abrupt way the encapsulated essential oil from the pores. The number of the discrete movements vs  
46  
47 locomotion time was calculated and depicted in Figure 4e, and is found to be very similar to the one  
48  
49 obtained from the video analysis of the experiment performed under the same conditions, previously  
50  
51 presented in Figure 2i.  
52  
53  
54  
55  
56  
57  
58  
59  
60  
61  
62  
63  
64  
65

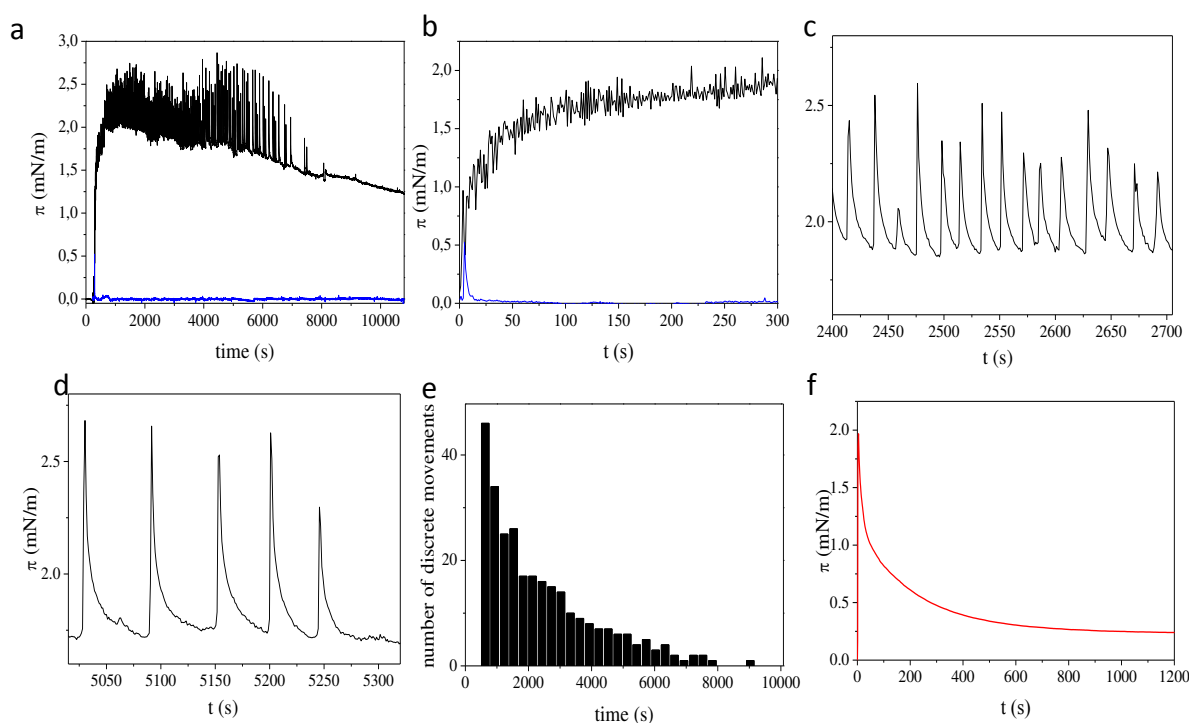


**Figure 4** Experiments of surface tension change connected with the locomotion of the composite films and intermittent motion analysis. **a**, Surface tension change vs. time measurements of CA only (blue line) and CA-PM (black line) Motor at air/water interface. **b**, Surface tension change vs. time measurements in the continuum motion region (black line). **c,d** Surface tension change vs. time measurements in the intermittent motion region. **e**, Number of discrete movements of the Motor at 5 min time intervals. **f**, Relaxation experiment of 0.6 mg of EO spread at air water interface.

In order to calculate the amount of the essential oil needed for a change in the water surface tension by 2 mN/m, different amounts of PM essential oil were spread at the free air water interface (without the Motor). From the obtained surface pressure vs area isotherms depicted analytically in supporting information **Figure S6** the calculated amount of PM essential oil was about 0.6 mg. In **Figure 4f** is shown the variation of the surface tension with the time, when 0.6 mg of PM essential oil was released onto the water surface at time zero. In this case the maximum change of surface tension of

1  
2  
3  
4  
5 2 mN/m was already reached after 4 s and then it tends to return to the starting value reaching a  
6  
7 plateau, a bit higher than zero, after few hundreds of seconds, due to the non-volatile components of the  
8  
9 PM essential oil. These, as expected, are much faster dynamics than the ones of the release and  
10  
11 relaxation when the composite material is placed on the water surface since in the latter case the CA  
12  
13 matrix controls the PM essential oil release (note that the produced Motors contain 6.7 mg of PM). Due  
14  
15 to this controlled release, and the simultaneous evaporation and dissolution mechanisms, a much higher  
16  
17 amount of PM essential oil than 0.6 mg needs to be exerted from the matrix in order to eventually be  
18  
19 reached a change in the water surface tension of 2 mN/m.  
20  
21  
22  
23  
24  
25  
26  
27  
28

### 29 **3. Conclusions**

30  
31 Summarizing, in this work it was presented the development of a new natural porous composite  
32  
33 material, using a combination of cellulose acetate polymer with an essential oil, that showed self-  
34  
35 motion on water due to the “Marangoni effect”. The velocity duration of the natural composite are  
36  
37 higher compared to other propellants, that contain the propelled object themselves, reported until now.  
38  
39 The presented system is a versatile self-motor without the need of an external fuel reservoir or an added  
40  
41 boat to stimulate or support the composite. The mechanism of the locomotion was based on the slow  
42  
43 release of essential oil due to the highly porous matrix of the Motors, and its simultaneous evaporation  
44  
45 from the water surface, resulting in extended surface tension gradient, enabling the prolonged  
46  
47 movement of the Motor. The Motors stop moving when all the PM oil is released from their pores. An  
48  
49 amount of 6.7  $\mu\text{l}$  of PM essential oil was able to move the Motors for 60 m in 4000 s (1 hour and 7  
50  
51 min) and for more than 75 m in 3 hours. A velocity of more than 10 cm/s was achieved at least for the  
52  
53 first 30 min of movement. It was also found that the surface tension change was very well correlated to  
54  
55 the kinetic energy variations of the Motors in time. The knowledge acquired in this work can be useful  
56  
57  
58  
59  
60  
61  
62  
63  
64  
65



1  
2  
3  
4  
5 in further studies of self-propelled bio-mimetic aquatic systems, and the obtained optimized and  
6  
7 prolonged motion can be used for developing technologies for drug delivery, energy harvesting, lab-on-  
8  
9 a-chip or other advanced applications.

#### 14 **4. Experimental Section**

15  
16  
17 *Incorporation of PM oil into CA and preparation of boats.* A solution of CA (5% w/v) and PM oil  
18  
19 (10% v/v) in acetone was prepared. The mixture was casted on a silicon wafer and the solvent was left  
20  
21 to evaporate. Then the film was detached from the substrate and cut in disc shapes with 14 mm  
22  
23 diameter, 55  $\mu\text{m}$  thickness and 10 mg weight.

24  
25  
26  
27 *Instrumentation.* A Park System AFM instrument (XE-100) was used in non-contact mode. The images  
28  
29 were acquired in air on an anti-vibration table (Table Stable TS-150) and within an acoustic enclosure.  
30  
31 Single-beam silicon cantilevers tips (PPP-NCHR-10) were used for the data acquisition with about less  
32  
33 than 10 nm nominal radius and 42 N/m elastic force constant for high sensitivity. The resonance  
34  
35 frequency was defined around 280 kHz and the scan rate was maintained at 0.2 Hz. SEM was carried  
36  
37 out using a JEOL JSM6490LA (Jeol, Tokyo, Japan) equipped with a W thermionic source working at  
38  
39 an acceleration voltage of 15 kV. Imaging has been obtained using secondary electrons. Due to the  
40  
41 nonconductive nature of the samples, they have been coated with a 10 nm gold layer using a  
42  
43 Cressington 108 Auto sputter coater (Cressington Scientific Instruments Inc, Cranberry Twp, PA).  
44  
45 Static surface isotherm and surface -area isotherms experiment were performed with a KSV 2000  
46  
47 Langmuir equipped with a platinum balance with 4  $\mu\text{N/m}$  of resolution. For the static surface  
48  
49 measurements, the Motors were placed in contact with the surface of 200 ml of Milli-Q water  
50  
51 (pH=7.55) contained in a circular glass Petri dish with an internal diameter of 14 cm. The surface -area  
52  
53 isotherms were performed on a PTFE trough with 280 ml of Milli-Q water as subphase. Wettability  
54  
55 measurements were carried out by sessile drop method using a DataPhysics OCAH 200 Contact Angle  
56  
57  
58  
59  
60  
61  
62  
63  
64  
65

Goniometer at laboratory conditions (temperature of 22-25 °C and relative humidity of 50-60%).

ImageJ analysis was used to calculate the number and the area of the open pores, the SEM images were processed to “binary images”, then find edges was selected from “process” and then “analyse particles” was selected where the number and the area of the particles were calculated.

*Locomotion analysis.* A glass Petri dish (diameter of 14 cm) was filled with 200 ml of Milli-Q water (pH=7.55). The Motor was positioned at the air/water interface and their motion was recorded by an industrial camera (Flea3 Point Grey). An automatic algorithm was designed to analyze the motion of the Motor. Each experiment has been recorded with the industrial camera at 25 fps and resolution of 600 x 600 pixels, RGB colors. The camera image plane was parallel to the water surface at a distance of about 30 cm. (We also calibrated the intrinsic and extrinsic camera parameters with a checkerboard pattern, a pixel side corresponds to about 0.24 mm on the water surface). For a better characterization of the motion both the translation and the self-rotation of the Motor have been taken into account. To set an orientation for the Motor we put a small black dot on the sample. More information is presented in Supporting Information **Figures S7 – S9**.

## Supporting Information

Supporting Information is available from the Wiley Online Library or from the authors.

## Acknowledgements

The Authors would like to thank Dr. Ilker S. Bayer for his useful discussions at the initial stages of this work and Prof. Vittorio Murino for his helpful discussions on the video analysis of the motion

Received:

Revised:

## References

1. Nakata, S., Y. Hayashima, *Journal of the Chemical Society-Faraday Transactions* **1998**, *94*, 3655.
2. Sempels, W., R. De Dier, H. Mizuno, J. Hofkens, J. Vermant, *Nat Commun* **2013**, *4*, 1757.
3. Gao, X., L. Jiang, *Nature* **2004**, *432*, 36.
4. Bush, J.W.M., D.L. Hu, M. Prakash, *Advances in Insect Physiology* **2007**, *34*, 117.
5. Dickinson, M., *Nature* **2003**, *424*, 621.
6. Hu, D.L., B. Chan, J.W. Bush, *Nature* **2003**, *424*, 663.
7. Bassik, N., B.T. Abebe, D.H. Gracias, *Langmuir* **2008**, *24*, 12158.
8. Ikura, Y.S., R. Tenno, H. Kitahata, N.J. Suematsu, S. Nakata, *J Phys Chem B* **2012**, *116*, 992.
9. Jin, H., A. Marmur, O. Ikkala, R.H.A. Ras, *Chemical Science* **2012**, *3*, 2526.
10. Kitahata, H., S. Hiromatsu, Y. Doi, S. Nakata, M.R. Islam, *Physical Chemistry Chemical Physics* **2004**, *6*, 2409.
11. Liu, X., J. Gao, Z. Xue, L. Chen, L. Lin, L. Jiang, S. Wang, *ACS Nano* **2012**, *6*, 5614.
12. Luo, C., H. Li, L. Qiao, X.C. Liu, *Microsystem Technologies-Micro-and Nanosystems-Information Storage and Processing Systems* **2012**, *18*, 1525.
13. Mou, F., C. Chen, H. Ma, Y. Yin, Q. Wu, J. Guan, *Angew Chem Int Ed Engl* **2013**, *52*, 7208.
14. Nagayama, M., S. Nakata, Y. Doi, Y. Hayashima, *Physica D-Nonlinear Phenomena* **2004**, *194*, 151.
15. Nakata, S., Y. Arima, *Colloids and Surfaces a-Physicochemical and Engineering Aspects* **2008**, *324*, 222.
16. Nakata, S., Y. Doi, Y. Hayashima, *Journal of Physical Chemistry B* **2002**, *106*, 11681.
17. Nakata, S., M. Hata, Y.S. Ikura, E. Heisler, A. Awazu, H. Kitahata, H. Nishimori, *Journal of Physical Chemistry C* **2013**, *117*, 24490.
18. Nakata, S., N. Kawagishi, M. Murakami, N.J. Suematsu, M. Nakamura, *Colloids and Surfaces a-Physicochemical and Engineering Aspects* **2009**, *349*, 74.
19. Nakata, S., K. Matsuo, *Langmuir* **2005**, *21*, 982.
20. Nakata, S., R. Tenno, Y.S. Ikura, *Chemical Physics Letters* **2011**, *514*, 159.
21. Restrepo-Perez, L., L. Soler, C.S. Martinez-Cisneros, S. Sanchez, O.G. Schmidt, *Lab Chip* **2014**, *14*, 1515.
22. Soh, S., K.J. Bishop, B.A. Grzybowski, *J Phys Chem B* **2008**, *112*, 10848.
23. Soler, L., V. Magdanz, V.M. Fomin, S. Sanchez, O.G. Schmidt, *ACS Nano* **2013**, *7*, 9611.
24. Wang, W., W.T. Duan, S. Ahmed, T.E. Mallouk, A. Sen, *Nano Today* **2013**, *8*, 531.
25. Wu, Y., Z. Wu, X. Lin, Q. He, J. Li, *ACS Nano* **2012**, *6*, 10910.
26. Guix, M., J. Orozco, M. Garcia, W. Gao, S. Sattayasamitsathit, A. Merkoci, A. Escarpa, J. Wang, *ACS Nano* **2012**, *6*, 4445.
27. Ikezoe, Y., G. Washino, T. Uemura, S. Kitagawa, H. Matsui, *Nat Mater* **2012**, *11*,
28. Pimienta, V., C. Antoine, *Current Opinion in Colloid & Interface Science* **2014**, *19*, 290.
29. Thomson, J., *The London, Edinburgh, and Dublin Philosophical Magazine of Journal of Science* **1855**, *X*, 330.
30. Harris, C., M. Stephens. *A combined corner and edge detector*. in *In Alvey vision conference*. **1988**. Manchester, UK.
31. Zhang, Z., *IEEE Trans. Pattern Analysis and Machine Intelligence* **2000**, *22*, 1330.
32. Canny, J., *IEEE Trans. Pattern Analysis and Machine Intelligence* **1986**, *8*, 679.
33. Ioannou, D., W. Huda, A.F. Laine, *Image and Vision Computing* **1999**, *17*, 15.
34. Nakata, S., Y. Iguchi, S. Ose, M. Kuboyama, T. Ishii, K. Yoshikawa, *Langmuir* **1997**, *13*, 4454.
35. Zhao, G., T.H. Seah, M. Pumera, *Chemistry* **2011**, *17*, 12020.
36. Cassie, A.B.D., S. Baxter, *Transactions of the Faraday Society* **1944**, *40*, 546.
37. Arneodo, C., A. Baszkin, J.P. Benoit, R. Fellous, C. Thies, *Colloids and Surfaces* **1988**, *34*, 159.

- 1
- 2
- 3
- 4
- 5 38. Parry, E.J., *The Chemistry of Essential Oils and Artificial Perfumes*. 4th ed. **1922**, London: Scott,
- 6 Greenwood and Son.
- 7 39. Fowkes, F.M., ed. *Hydrophobic surfaces*. **1969**, Academic Press: New York, USA.
- 8 40. Nalwa, H.S., ed. *Handbook of surfaces and interfaces of materials: surface and interface phenomena*.
- 9 **2001**, Academic Press: USA.
- 10 41. Suematsu, N.J., T. Sasaki, S. Nakata, H. Kitahata, *Langmuir* **2014**, *30*, 8101.
- 11 42. Nakata, S., J. Kirisaka, *J Phys Chem B* **2006**, *110*, 1856.
- 12 43. Burton, L.J., N. Cheng, C. Vega, J. Andres, J.W. Bush, *Bioinspir Biomim* **2013**, *8*, 044003.
- 13 44. Nakata, S., Y. Doi, H. Kitahata, *The Journal of Physical Chemistry B* **2005**, *109*, 1798.
- 14
- 15
- 16
- 17
- 18
- 19
- 20
- 21
- 22
- 23
- 24
- 25
- 26
- 27
- 28
- 29
- 30
- 31
- 32
- 33
- 34
- 35
- 36
- 37
- 38
- 39
- 40
- 41
- 42
- 43
- 44
- 45
- 46
- 47
- 48
- 49
- 50
- 51
- 52
- 53
- 54
- 55
- 56
- 57
- 58
- 59
- 60
- 61
- 62
- 63
- 64
- 65

Supporting Information

[Click here to download Supporting Information: Bio-mimetic locomotion on water of a porous natural polymeric composite Supporting Info.](#)